processes

MDPI

Article

Multiscale Gas Flow Mechanisms in Ultra-Deep Fractured Tight Sandstone Reservoirs with Water Invasion

Liandong Tang [1,2,3], Yongbin Zhang [1,2,3], Xueni Chen [4], Qihui Zhang [1,2,3], Mingjun Chen [4,*], Xuehao Pei [1,2,3], Yili Kang [4], Yiguo Zhang [1,2,3], Xingyu Tang [4], Bihui Zhou [1,2,3], Jun Li [1,2,3], Pandong Tian [1,2,3] and Di Wu [1,2,3]

1 R&D Center for Ultra-Deep Complex Reservoir Exploration and Development, CNPC, Korla 841000, China; tangld-tlm@petrochina.com.cn (L.T.); zyongb-tlm@petrochina.com.cn (Y.Z.)
2 Engineering Research Center for Ultra-Deep Complex Reservoir Exploration and Development, Xinjiang Uygur Autonomous Region, Korla 841000, China
3 Xinjiang Key Laboratory of Ultra-Deep Oil and Gas, Korla 841000, China
4 State Key Laboratory of Oil and Gas Reservoir Geology and Exploitation, Southwest Petroleum University, Chengdu 610500, China
* Correspondence: chenmj1026@163.com

Abstract

Ultra-deep fractured tight sandstone reservoirs are key targets for natural gas development, where gas flow is controlled by pore structure, capillary forces, and water saturation. Using the ultra-deep tight sandstones from the Tarim Basin as study object, this paper investigates the gas flow behavior in matrix and fractured cores under high-temperature, high-pressure, and various water saturation conditions. The controlling factors of gas flow are investigated through scanning electron microscopy, casting thin-section, and high-pressure mercury intrusion measurements. The results show that increasing the water saturation can significantly reduce the permeability. The permeability of matrix and fractured cores decreases by 71.15% and 79.67%, respectively, when water saturation reaches 50%. The gas slippage is negligible, but the effect of gas threshold pressure is significant, which is primarily controlled by the pore structure and water saturation. The threshold pressure gradient of gas flow ranges from 0.0004 to 0.8762 MPa/cm, with the matrix cores exhibiting values approximately 13.21 times higher than the fractured cores. The water phase preferentially occupies the larger pores, forcing gas flow to rely on the finer pores. The pores with a maximum radius of 0.21 μm require 0.66 MPa of driving pressure for gas, whereas pores with a median radius of 0.033 μm require 4.18 MPa. The fracture networks can significantly reduce the lower limit for gas flow, serving as the key flow channels for the efficient development of ultra-deep tight sandstone gas. These findings not only reveal the gas flow mechanisms under water invasion but also provide theoretical and practical guidance for enhancing gas recovery from ultra-deep tight sandstone reservoirs.

Keywords: ultra-deep tight sandstone gas reservoir; permeability; multiscale pore structure; nonlinear gas flow; threshold pressure gradient

check for updates

Academic Editors: Qingbang Meng and Kejun Dong

Received: 25 September 2025
Revised: 4 November 2025
Accepted: 5 November 2025
Published: 7 November 2025

Citation: Tang, L.; Zhang, Y.; Chen, X.; Zhang, Q.; Chen, M.; Pei, X.; Kang, Y.; Zhang, Y.; Tang, X.; Zhou, B.; et al. Multiscale Gas Flow Mechanisms in Ultra-Deep Fractured Tight Sandstone Reservoirs with Water Invasion. *Processes* **2025**, *13*, 3596. https://doi.org/10.3390/pr13113596

Copyright: © 2025 by the authors. Licensee MDPI, Basel, Switzerland. This article is an open access article distributed under the terms and conditions of the Creative Commons Attribution (CC BY) license (https://creativecommons.org/licenses/by/4.0/).

1. Introduction

Ultra-deep fractured tight sandstone reservoirs represent a key frontier in unconventional gas exploration and development, and their resource potential plays a significant role in the global gas supply. In recent years, advances in exploration and production technologies have enabled the discovery of numerous ultra-deep tight sandstone gas reservoirs with burial depths exceeding 6000 m in basins such as the Tarim. These reservoirs possess

substantial resource potential and show promising development prospects, making them the primary targets for future tight sandstone gas exploration [1–3]. These reservoirs are characterized by high temperatures, pressures, and in situ stresses. The pores are strongly heterogeneous, with a tight matrix and very small pores coexisting with the pervasive natural fractures. This produces a classic matrix–fracture dual-porosity system [4–7]. This attribute results in a complex and strongly nonlinear gas flow behavior that departs from the linear flow regimes of conventional reservoirs. Meanwhile, the active aquifers and water invasion are common in many ultra-deep fractured tight sandstone reservoirs. It complicates gas flow during production and poses serious challenges to enhancing gas recovery [8–10]. Therefore, a systematic understanding of gas flow and mobilization mechanisms under water invasion conditions in ultra-deep fractured tight sandstones is both theoretically important and practically valuable. Furthermore, fluid flow in ultra-deep fractured tight sandstone reservoirs not only governs gas migration but also impacts reservoir modification and environmental evolution, such as fracture propagation, mineral dissolution–precipitation, and stress redistribution during production. Multiphase flow can alter fracture apertures and local stress states, thereby influencing the long-term stability and productivity of the reservoir [11,12].

In recent years, water invasion in gas reservoirs has been the focus of extensive research. Persoff et al. investigated water invasion and its disturbance to flow in porous media [13]. Fang et al. examined the influence of various controlling factors on water invasion through core experiments [14,15]. Research on gas flow under water invasion encompasses extensive physical experiments as well as a rich body of theoretical and numerical modeling. In terms of experimental methods, the JBN method has become a classical approach for determining relative permeability [16]. Generally, the steady-state and unsteady-state methods are used to obtain permeability curves. Experimental and theoretical studies have shown that the surface roughness, lithology, wettability, displacement pattern, temperature, and effective stress can all significantly influence the permeability of tight sandstones and the measurement and characterization of relative permeability [17–21].

Overall, extensive studies have been conducted worldwide on gas flow behavior under water invasion from both experimental and theoretical perspectives. The gas water flow behavior and capillary interactions in ultra-tight formations directly affect permeability evolution and production performance [22–24]. However, almost all experiments have been performed without considering the in situ reservoir temperature and pressure. Permeability is strongly influenced by temperature and pressure, and permeability decreases with increasing effective stress and temperature, resulting in significant differences among the results obtained under different experimental conditions [25,26]. Therefore, the gas flow experiments at various water saturations should be carried out under temperature and pressure conditions corresponding to the actual reservoir environment. In addition, the permeability of a tight sandstone is closely related to its pore structure and mineral composition [27–30]. In addition, the analysis of water invasion effects on gas permeability must be integrated with the microscopic structure and mineralogical characteristics of the samples.

Moreover, a series of experiments have shown that gas seepage curves do not pass through the origin and exhibit nonlinear behavior at the low flow rates, gradually becoming linear as flow rates increase [31–33]. This indicates the presence of a threshold pressure gradient (TPG) effect in the tight sandstone gas reservoirs, which has a significant impact on gas production. Recent modeling and micro-scale visualization studies have provided new insights into the nonlinear seepage and TPG mechanisms in tight formations [34–37]. The TPG is not only governed by pore structure and wettability but also by multiphase interactions, stress sensitivity, and temperature-pressure coupling effects. These advancements

establish a theoretical basis for quantifying the pressure threshold required for gas mobilization under complex reservoir conditions [38–42]. If the impact of TPG on water-bearing sandstone gas reservoirs is ignored, the evaluation of well productivity may be inaccurate. Zhu et al. reported that the TPG increases with decreasing permeability or increasing water saturation, although no explicit correlation was proposed [43,44]. Therefore, it is essential to further investigate the effect of different water saturations on the TPG of tight sandstones. Although many studies have investigated gas water two-phase flow in tight sandstones, a comprehensive understanding of gas flow mechanisms under water invasion remains limited, particularly under high-temperature and high-pressure conditions representative of ultra-deep reservoirs. Existing research mainly focuses on conventional or shallow tight sandstones, while the coupling effects of water saturation, pore structure, and TPG under realistic formation conditions have not been systematically addressed.

This study focuses on the ultra-deep fractured tight sandstone reservoirs in the Kelasu structural belt of the Tarim Basin. The gas flow behavior of matrix and fractured cores under various water saturations was examined. Combined with the analyses of gas slippage and multiscale flow pathways, this work clarifies the controlling factors and effective conditions for gas flow under water invasion. The novelty of this study lies in its comprehensive investigation of gas flow behavior under actual in situ temperature and pressure conditions, which have been largely overlooked in previous studies. Moreover, the experimental design integrates varying water saturations to quantitatively assess their influence on the TPG and multiscale flow mechanisms. By coupling core experiments with detailed pore scale characterization, this work provides new and distinct insights into nonlinear gas transport in ultra-deep fractured tight sandstones, establishing a solid foundation for improved understanding and modeling of gas flow processes in deep unconventional reservoirs.

2. Experimental Materials and Methods

2.1. Experimental Materials

The experimental samples were collected from the Bashijiqike Formation in the Kelasu structural belt of the Tarim Basin, with burial depths ranging from 5835.0 to 6958.5 m. The study area is characterized as an ultra-deep tight sandstone gas reservoir. The Kelasu structural belt, located in the Kuqa Depression, is a major near-EW trending structural zone characterized by east–west segmentation and north–south zoning. From west to east, it can be subdivided into the Awate, Bozi, Dabei, Keshen, and Kela segments. In this study, matrix and fractured sandstone samples were collected from the Bozi, Dabei, and Keshen blocks for experimental investigation. The basic properties of the experimental samples, including length, diameter, porosity, and permeability, are summarized in Table 1.

Table 1. Basic parameters of the experimental samples.

Sample Type	Sample ID	Length (cm)	Diameter (cm)	In Situ Porosity (%)	In Situ Permeability (mD)
Matrix Cores	BZ-1	3.08	2.55	2.85	0.00256
	DB-1	5.54	2.55	2.68	0.00077
	KS-1	3.52	2.52	6.27	0.00174
Fractured Cores	BZ-2	3.11	2.54	3.05	1.18417
	DB-2	5.58	2.54	2.82	1.01876
	KS-2	5.02	2.55	5.17	2.00046

As shown in Figure 1, the water contact angles of sandstone samples from the Bozi, Dabei, and Keshen blocks are 25.74°, 24.50°, and 20.86°, respectively, all of which indicate strong hydrophilic wettability.

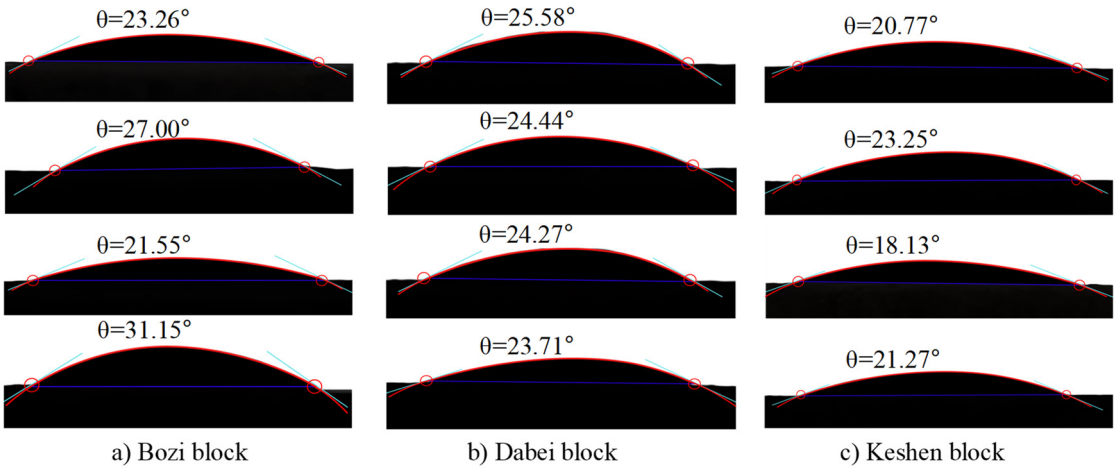


Figure 1. Water contact angles of tight sandstone samples.

According to the PVT reports and natural gas analysis reports of the study area, the Keshen block is classified as a dry gas reservoir, the Dabei block as a wet gas reservoir, and the Bozi block as a condensate gas reservoir. Therefore, different experimental gases were used for the sandstone samples from the three blocks, with their specific compositions summarized in Table 2. The differences in gas composition may slightly affect flow behavior. Dry gas exhibits lower viscosity and higher mobility. In contrast, wet and condensate gases contain heavier hydrocarbon components, which increase viscosity and capillary effects, thereby elevating the TPG and reducing gas flow capacity.

Table 2. Gas compositions used in the experiments.

Block	Gas Type	Simulated Gas Composition
Keshen	Dry gas	100% CH_4
Dabei	Wet gas	100% CH_4
Bozi	Condensate gas	86.7% Methane (CH_4) + 13.3% Ethane (C_2H_6)

2.2. Experimental Methods

A high-temperature and high-pressure multiscale seepage apparatus was employed in this study, as illustrated in Figure 2. The system integrates pressurization and flow measurement, with the outlet flowmeter and outlet pressure pump integrated into a single metering unit. The apparatus is capable of operating at pressures up to 200 MPa and temperatures up to 200 °C.

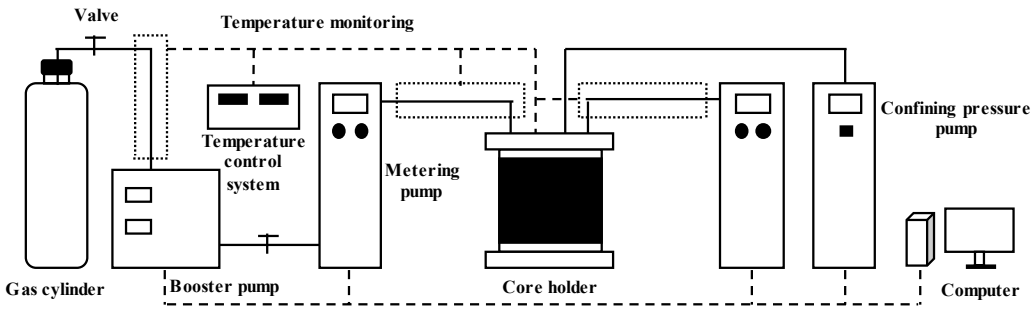


Figure 2. Schematic diagram of the high-temperature and high-pressure multiscale seepage apparatus.

Using this experimental system, the effects of different water saturations on gas flow capacity were investigated under in situ temperature and pressure conditions. The experimental water saturations were set at 0, 15%, 30%, and 50%. The experimental gases

were the simulated gas mixtures corresponding to the different reservoir blocks. The experimental procedure consisted of the following steps:

(1) Sample preparation. The samples obtained from drilling were subjected to oil and salt removal, followed by drying in an oven at 110 °C for 24 h before use.
(2) Pre-experiment preparation. The sample was mounted in the core holder, and the gas cylinder was opened. The confining pressure, inlet pressure, and outlet pressure were then loaded to the initial target values, while the temperature was increased to the specified level. The pressure and temperature conditions varied among the Bozi, Dabei, and Keshen blocks, with the specific values listed in Table 3.
(3) Gas seepage experiments. With the inlet pressure held constant, the outlet pressure was gradually reduced in steps. The pressure difference between the inlet and outlet was controlled within 5 MPa for matrix cores and within 1 MPa for fractured cores corresponding to their respective permeability levels and ensuring stable gas flow under high-temperature and high-pressure conditions. The outlet flow was subsequently monitored using the metering pump. Equilibrium was confirmed when the outlet flow rate and pressure differential remained constant for more than 30 min, indicating that transient effects had subsided.
(4) After gas seepage experiment, the gas cylinder was closed and the sample was removed.
(5) Establishment of different water saturations. Different target water saturations were achieved using the imbibition method, after which steps (2–4) were repeated for each water saturation level. Specifically, a 3 wt% KCl solution was used as the imbibition fluid. The core surface was gently rolled on fibers soaked with the solution, and its mass was continuously measured in real time. The amount of absorbed water was converted into the equivalent initial water saturation of the core. The saturated cores were then placed in a vacuum chamber to ensure a uniform distribution of the water phase prior to the gas flow experiments.
(6) Data processing. The experimental data were analyzed to quantify the effects of water saturation on the gas seepage capacity of both matrix and fractured cores.

Table 3. Experimental temperature and pressure conditions for tight sandstone samples.

Block	Temperature (°C)	Inlet Pressure (MPa)	Outlet Pressure (MPa)	Confining Pressure (MPa)
BZ	121.0	92.5	92.5	133.1
DB	147.5	111.9	111.9	158.2
KS	170.0	120.0	120.0	152.6

3. Results

3.1. Gas Flow in Matrix Samples Under Different Water Saturations

The gas flow characteristics of matrix cores from the Bozi, Dabei, and Keshen blocks under different water saturations are shown in Figure 3. The relationship between gas flow rate and pressure-squared gradient exhibits a predominantly linear trend. Under dry conditions, the gas flow is approximately linear with the pressure-squared gradient, so the nonlinear effect can be neglected. However, as the water saturation increases, significant flow restrictions appear in the low-pressure gradient region, and the nonlinear flow characteristics become more pronounced.

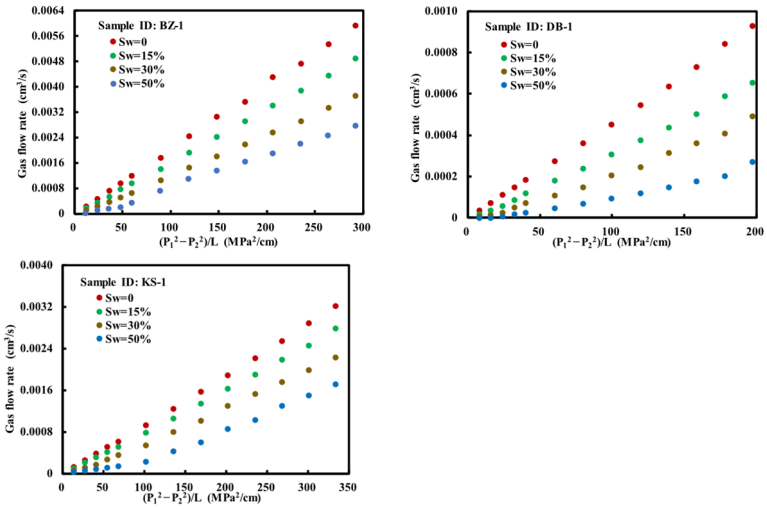


Figure 3. Gas flow characteristics of matrix samples under different water saturations.

As shown in Figure 4a, the permeability of matrix cores decreases markedly with increasing water saturation. When the water saturation increases from 0% to 50%, the permeability declines by approximately 71.15%, indicating that the water phase progressively occupies the effective flow channels and substantially reduces the gas flow capacity. Moreover, the differences in permeability decline are observed among the three research blocks. The cores with lower permeability exhibit stronger nonlinear effects, which are reflected in the higher TPG and more severe flow restrictions.

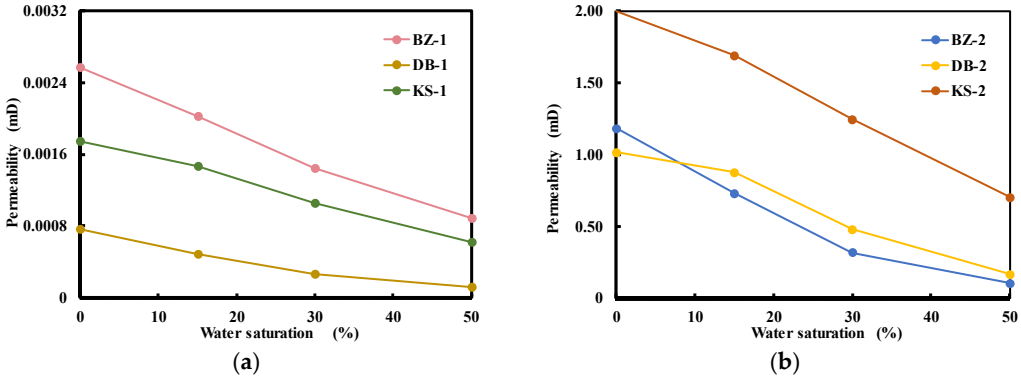


Figure 4. Variation in core permeability with water saturation. (**a**) Matrix cores; (**b**) Fractured cores.

In summary, the gas flow capacity of matrix cores under water-bearing conditions is highly sensitive to the water saturation, with nonlinear flow behavior being more prominent in the lower-permeability samples.

3.2. Gas Flow in Fractured Samples Under Different Water Saturations

The gas seepage results of fractured cores under different water saturations are shown in Figure 5. Overall, the relationship between gas flow rate and pressure-squared gradient shows an approximately linear trend. Under the dry conditions, the gas flow is nearly linear with the pressure-squared gradient, and the nonlinear effects can be neglected. With the increasing water saturation, the flow restriction becomes evident in the low pressure-gradient region, and the TPG increases. However, the overall magnitude is lower than the matrix cores, indicating that the fractures can still provide relatively unimpeded flow pathways even under high water saturation.

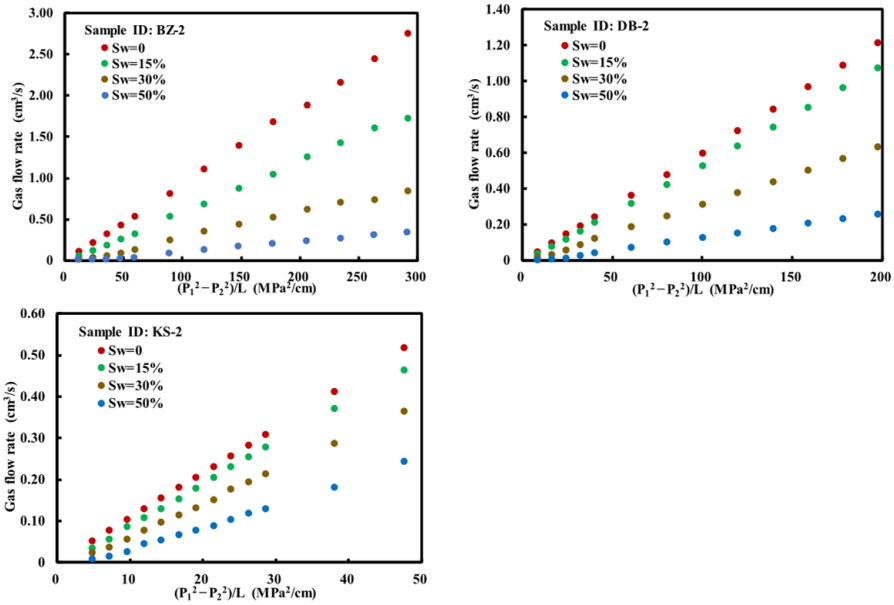


Figure 5. Gas flow characteristics of fractured sandstone samples under different water saturations.

The variation in permeability with water saturation for the fractured cores is shown in Figure 4b. As water saturation increases from 0% to 50%, the permeability of fractured cores decreases by 79.67%, suggesting that the water progressively accumulates within the fracture space and weakens the gas flow capacity. Nevertheless, compared with the matrix cores, the fractured cores exhibit the lower TPG and the weaker nonlinear flow characteristics under high water saturation. It is indicated that the fracture-dominated large-scale flow channels can provide sustained conductive pathways for gas, thereby reducing the degree to which fractured cores are influenced by the water phase.

4. Discussion

4.1. Impact of Gas Slippage on Flow Behavior

Under the low displacement pressure conditions, the relationships between the gas flow rate and the pressure-squared gradient for both matrix and fractured cores exhibited the concave-upward trend. These nonlinear flow characteristics were primarily governed by the pore structure and water saturation, rather than by the gas slippage. In addition, a simplified calculation of the Knudsen number was conducted, revealing that the mean free path of gas molecules is much smaller than the pore diameter, indicating that the flow is dominated by the continuum regime. Therefore, under in situ high-temperature and high-pressure conditions, the gas slippage effect in the core flow experiments can be reasonably neglected. As shown in Figure 6, the permeability of both matrix and fractured cores decreased progressively with the declining pore pressure, without exhibiting the typical increase expected in the presence of gas slippage. This trend further confirms that, within the pore pressure range investigated, the contribution of gas slippage effects to flow behavior is negligible.

In summary, for both matrix and fractured cores under the in situ conditions of ultra-deep tight sandstone reservoirs, the gas slippage exerts only a minimal influence on gas flow capacity. The observed nonlinear flow behavior is instead attributable to the TPG and the progressive occupation of effective flow channels by the water phase.

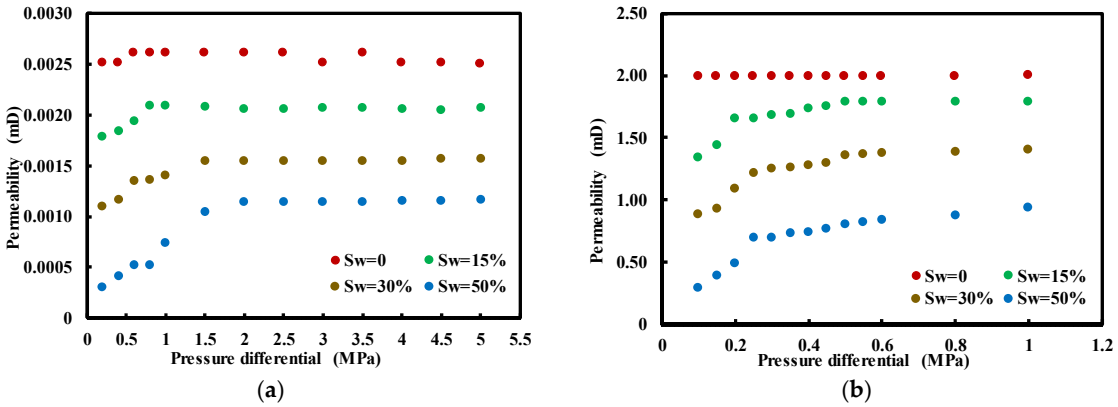


Figure 6. Relationship between permeability and displacement pressure difference. (**a**) matrix cores; (**b**) fractured cores.

4.2. Threshold Pressure Gradient in Nonlinear Gas Flow

Figures 7 and 8 illustrate the variation in TPG and its incremental changes under different water saturations for samples from the three research blocks. The TPG was indirectly derived from the relationship between gas flow rate and the pressure-squared gradient. The results show that gas flow in the fractured low-porosity sandstones generally exhibits a threshold pressure effect, with TPG ranging from 0.0004 to 0.8762 MPa/cm. This effect represents one of the dominant mechanisms governing nonlinear gas flow in tight sandstones.

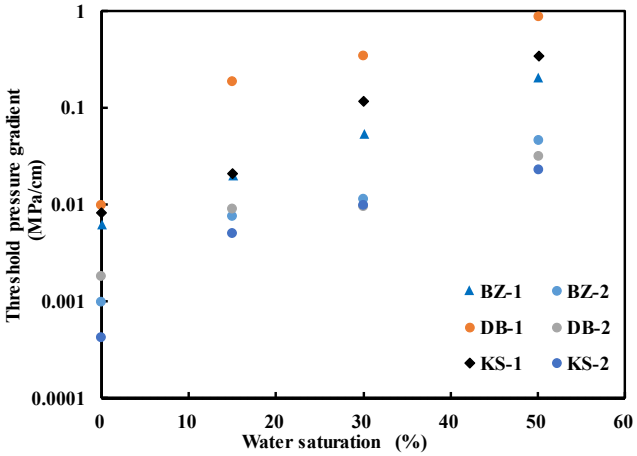


Figure 7. Variation in TPG with water saturation for different tight sandstones.

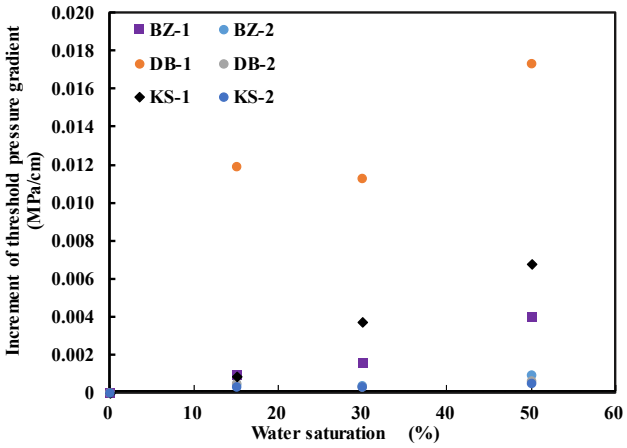


Figure 8. Variation in incremental TPG with water saturation for different tight sandstones.

Overall, the TPG increased markedly with the increasing rock tightness and higher water saturation. This phenomenon arises because the water phase progressively occupies pore or fracture spaces, restricting gas flow pathways and elevating the critical driving force required to overcome the capillary forces and interfacial resistance.

A direct comparison between the matrix and fractured cores further highlights the differences. At the same water saturation, the TPG of matrix cores was approximately 2.70–35.78 times higher than that of the fractured cores, with an average of 13.21 times. The results clearly indicate that the large-scale flow channels provided by fractures significantly attenuate the threshold pressure effect, whereas matrix cores are more susceptible to pore structure and water distribution. Notably, under high water saturation, the nonlinear flow characteristics became more pronounced in the matrix cores, while the fractured cores maintained relatively lower TPG and weaker flow restrictions.

In summary, the TPG plays a pivotal role in controlling the nonlinear gas flow in tight sandstones. Its magnitude is not only governed by the rock compactness but also strongly influenced by the water saturation, and the effect varies substantially between the matrix and fractured cores. Furthermore, the influence of geological factors such as temperature, pressure, and effective stress plays a crucial role in gas flow behavior of ultra-deep tight sandstones. Previous studies have shown that increasing temperature and confining pressure generally decrease permeability and enhance nonlinearity due to compaction and fluid rock interactions [45,46]. The present results are consistent with these findings, confirming that the coupled effects of high temperature, high pressure, and strong rock compaction intensify the TPG and restrict gas mobility in ultra-deep reservoirs.

4.3. Multiscale Gas Flow Mechanisms

Gas flow in tight sandstone reservoirs is constrained by multiple factors, primarily including the multiscale structural characteristics of pores and fractures, pore connectivity, and the distribution and evolution of the water phase. Experimental results demonstrate that the gas flow capacity depends not only on the pore-throat size and connectivity, but is also significantly influenced by the TPG and the extent of water phase occupancy.

As shown in the scanning electron microscopy (SEM) (Carl Zeiss Microscopy GmbH, Jena, Germany) images in Figure 9 and the casting thin-section (CTS) (Leica Microsystems GmbH, Wetzlar, Germany) observations in Figure 10, the sandstone matrix is characterized by low porosity, poor connectivity, and pronounced capillary effects. The pore sizes range from 0.01 mm to 0.25 mm, with an average porosity of approximately 3.3%. The coordination numbers of the pores are low, indicating poor pore connectivity. The predominant pore types include intergranular pores, intragranular pores, and micro fractures. The intergranular pores are often slit-like or irregular and are frequently surrounded or filled by the clay minerals, resulting in the loss of effective flow capacity, especially under water invasion. The intragranular pores are locally present but exhibit limited connectivity with surrounding pores. The micro fractures can be observed in certain samples, yet they are often discontinuous or partially filled with clay minerals. Such pore structure characteristics indicate that the gas flow through the matrix must overcome the substantial capillary forces. Meanwhile, the water phase accumulation can further exacerbate flow restrictions under high water saturation conditions.

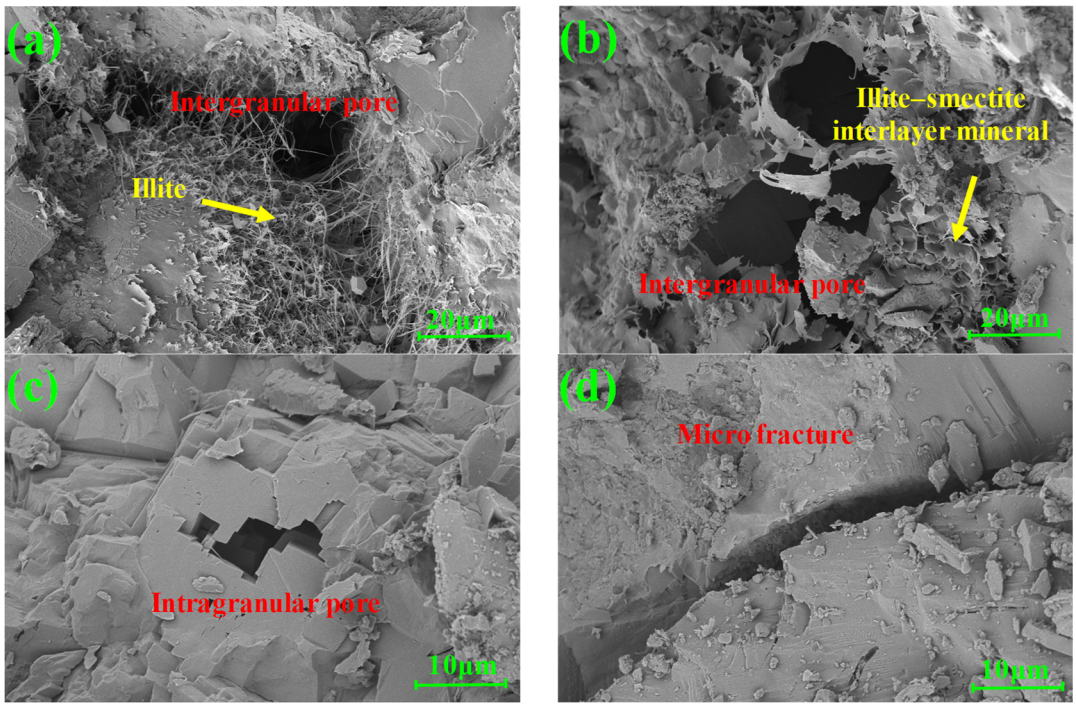


Figure 9. Scanning electron microscopy images of tight sandstone samples. (**a**) Intergranular pore and illite; (**b**) Intergranular pore and illite-smectite interlayer mineral; (**c**) Intragranular pore; (**d**) Micro fracture.

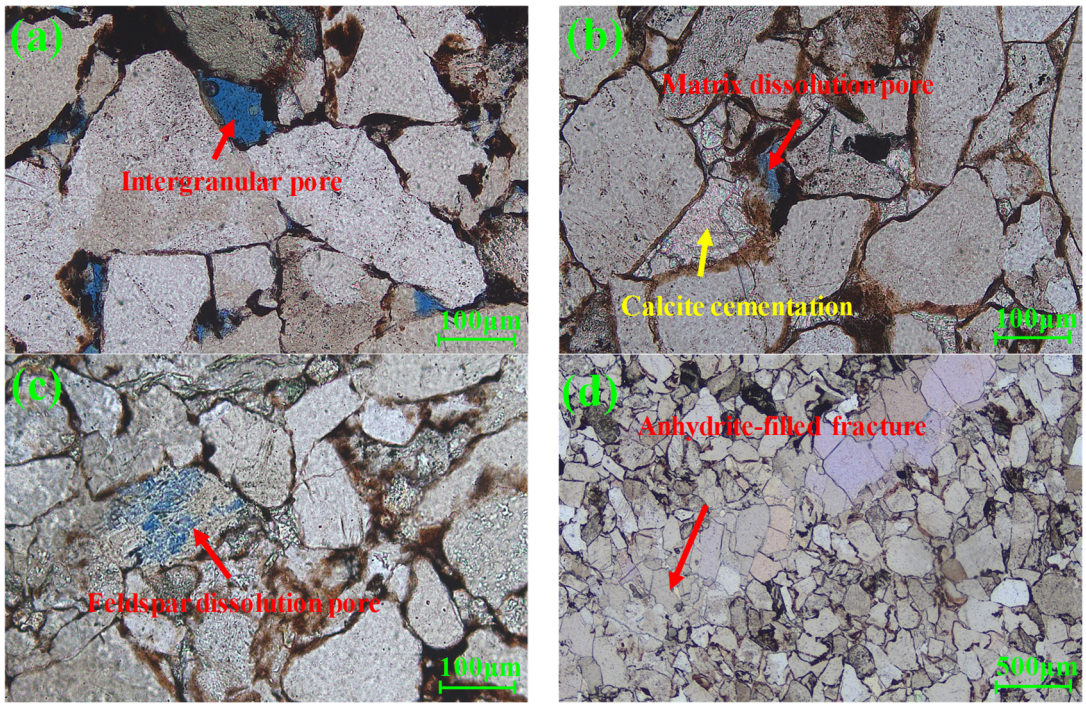


Figure 10. Casting thin-section images of tight sandstone samples (under plane-polarized light). (**a**) Intergranular pore; (**b**) Matrix dissolution pore and calcite cementation; (**c**) Feldspar dissolution pore; (**d**) Anhydrite-filled fracture.

Mineralogical analysis indicates that quartz is the dominant mineral, with an average proportion of 44.76%, followed by lithic fragments and feldspar. The clay mineral content ranges from 3% to 9%, primarily consisting of illite and illite-smectite interlayer mineral.

These minerals exhibit strong hydrophilicity and water absorption capacity, which is conductive to the formation of adsorbed water films along pore-throat surfaces.

The reduction in the effective pore-throat radius (25.65–44.90 nm) corresponds to the thickness of the adsorbed water film formed on the pore surfaces after water invasion. This value was calculated using the equilibrium water film thickness model, assuming a uniform distribution of the film along the pore walls. The formation of these water films significantly reduces the effective pore-throat radius, enhances capillary forces, and aggravates the discontinuity of gas flow. As a result, the two-phase flow is highly susceptible to water blocking and Jamin effects, leading to persistently high bound water saturation.

Overall, the gas flow in the ultra-deep tight sandstones is governed by a coupled pore-scale processes. The initial water saturation establishes wetting films on mineral surfaces. The continued water invasion drives capillary imbibition that thickens these films and redistributes water into the smallest pores and throats. This redistribution produces water blocking damage at critical constrictions and promotes bubble snap-off, yielding intermittent gas pathways. The combined outcome is a substantial reduction in gas flow capacity, manifested as the elevated TPG and the more pronounced nonlinear gas flow behavior.

4.4. Effective Flow Conditions of Ultra-Deep Tight Sandstone Gas

The relationship between water capillary pressure, pore radius, and water saturation offers critical insights into the effective conditions for gas flow in the ultra-deep tight sandstone reservoirs. As shown in Figure 11, with increasing water saturation, the water phase preferentially invades and occupies the larger pores, resulting in a gradual decrease in water capillary pressure. The preferential occupation of large pores by water forces the gas to migrate primarily through finer pores within the matrix, significantly increasing the difficulty of gas flow.

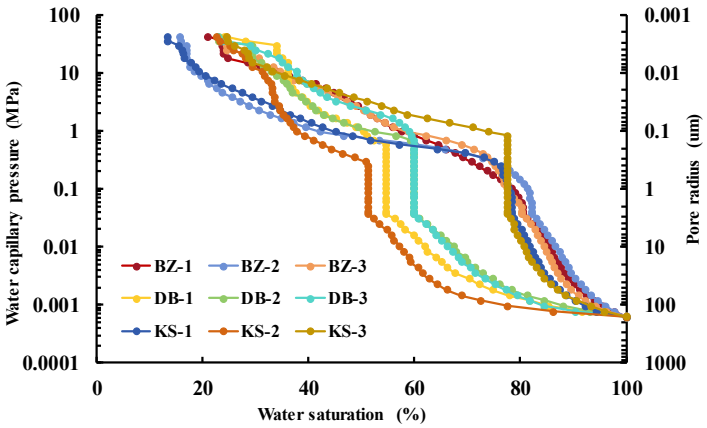


Figure 11. Relationship between water capillary pressure, pore radius, and water saturation.

Experimental results can further support the above observation. The gas flow in pores with an average maximum radius of 0.21 μm requires a minimum displacement pressure of only 0.66 MPa, whereas pores with an average median radius of 0.033 μm demand as high as 4.18 MPa. These findings indicate that although large pores can form effective flow channels under relatively low displacement pressures, they are more prone to being blocked by the water at high saturations, thereby limiting gas flow. In contrast, the abundant fine pores in the matrix exhibit high capillary pressures and require substantial driving pressure, rendering them less effective under practical reservoir conditions.

The matrix cores generally exhibit a relatively high threshold for gas flow. In contrast, the fractures provide large pore channels, enhancing the connectivity and lowering the

critical pressure required for the effective gas flow. The above observations highlight the crucial role of fractures in facilitating gas flow under water-bearing conditions. It should be noted that the experimental results obtained in this study are applicable to the steady state flow stage. While steady state flow characteristics provide the foundation for long term reservoir evaluation, transient flow dominates during the early production stage of ultra-low-permeability reservoirs. An advanced transient-analysis technique can effectively distinguish the respective contributions of the matrix and fracture systems under high stress conditions, refine the interpretation of pressure responses, and quantify stress sensitivity effects on fracture conductivity, thereby supporting production optimization [47].

Simultaneously, the experimental measurements confirmed the presence of significant TPG under high water saturation conditions and provide guidance for field-scale operations. From an engineering perspective, an appropriate production pressure drawdown should exceed the measured lower limit of TPG to initiate gas flow while avoiding excessive pressure drops that may induce stress sensitivity. In addition, optimizing fracture design to enlarge the drainage area and improve connectivity is crucial for enhancing gas recovery. It should be noted that these results are based on core scale experiments and require further validation at the reservoir scale under in situ conditions.

5. Conclusions

Globally, tight sandstone gas development is steadily advancing into deeper formations to ensure resource replacement. According to industry trends, the average extraction depth is increasing by approximately 20–40 m per year. This progression towards deeper and tighter reservoirs makes it increasingly critical to understand the multiscale gas flow behavior and TPG in ultra-deep environments. The main findings of this study are summarized as follows:

(1) The water saturation has a significant impact on the permeability of ultra-deep tight sandstones. As water saturation increases, the permeability of both matrix and fractured cores decreases markedly. When the water saturation increases from 0% to 50%, the permeability of matrix and fractured cores decreases by 71.15% and 79.67%, respectively, indicating a strong blocking effect of the water phase on gas flow.

(2) Under the in situ high-temperature and high-pressure conditions, both the matrix and fractured cores demonstrate an absence of gas slippage effect. The relationship between the gas flow rate and pressure-squared gradient transitions from a concave curve to nearly linear behavior, suggesting that nonlinear gas flow is primarily controlled by the tight pore structure and increasing water saturation.

(3) The TPG of ultra-deep tight sandstones ranges from 0.0004 to 0.8762 MPa/cm and increases significantly with rock compaction and water saturation. Under the same water saturation, the TPG of matrix cores is approximately 13.21 times higher than that of fractured cores, indicating that the fractures can effectively reduce the critical pressure required for gas flow.

(4) The water phase can preferentially occupy the larger pores, forcing the gas flow to rely on finer pores. The pores with a maximum radius of 0.21 μm require 0.66 MPa of driving pressure, whereas pores with a median radius of 0.033 μm require about 4.18 MPa. This indicates that the fracture networks can significantly reduce the lower limit for gas flow and serve as the primary flow channels for efficient development of ultra-deep tight sandstone gas.

Author Contributions: Conceptualization, L.T., Y.Z. (Yongbin Zhang), Y.Z. (Yiguo Zhang) and P.T.; methodology, L.T., Y.Z. (Yongbin Zhang), Q.Z., M.C., Y.K., X.T., B.Z., P.T. and D.W.; software, J.L. and D.W.; formal analysis, X.C. and X.P.; resources, L.T., Q.Z., M.C., X.P., Y.K., Y.Z. (Yiguo Zhang)

and B.Z.; data curation, Y.Z. (Yongbin Zhang), X.T. and J.L.; writing—original draft preparation, X.C.; writing—review and editing, X.C., M.C., Y.K. and X.T. All authors have read and agreed to the published version of the manuscript.

Funding: This research was supported by the CNPC Youth Science and Technology Project (No. Q202501.06) and the Project of R&D Center for Ultra Deep Complex Reservoir Exploration and Development, CNPC (No. YF202408.01).

Data Availability Statement: The original contributions presented in this study are included in the article. Further inquiries can be directed to the corresponding authors.

Conflicts of Interest: Authors Liandong Tang, Yongbin Zhang, Qihui Zhang, Xuehao Pei, Yiguo Zhang, Bihui Zhou, Jun Li, Pandong Tian and Di Wu were employed by R&D Center for Ultra-Deep Complex Reservoir Exploration and Development, China National Petroleum Corporation (CNPC). The remaining authors declare that the research was conducted in the absence of any commercial or financial relationships that could be construed as a potential conflict of interest.

References

1. Zou, C.; Zhu, R.; Liu, K.; Su, L.; Bai, B.; Zhang, X.; Yuan, X.; Wang, J. Tight gas sandstone reservoirs in China: Characteristics and recognition criteria. *J. Pet. Sci. Eng.* **2012**, *88*, 82–91. [CrossRef]
2. Jia, A.; Wei, Y.; Guo, Z.; Wang, G.; Meng, D.; Huang, S. Development status and prospect of tight sandstone gas in China. *Nat. Gas Ind. B* **2022**, *9*, 467–476. [CrossRef]
3. Liu, Z.; Song, X.; Fu, X.; Luo, X.; Wang, H. Energy Production Potential of Ultra-Deep Reservoirs in Keshen Gas Field, Tarim Basin: From the Perspective of Prediction of Effective Reservoir Rocks. *Energies* **2025**, *18*, 2913. [CrossRef]
4. Zhang, H.; Zhang, R. Characterization and evaluation of ultra-deep fracture-pore tight sandstone reservoirs: A case study of Cretaceous Bashijiqike Formation in Kelasu tectonic zone in Kuqa foreland basin, Tarim, NW China. *Pet. Explor. Dev.* **2014**, *41*, 175–184. [CrossRef]
5. Zhang, R.; Yang, H.; Wang, J.; Shou, J.; Zeng, Q.; Liu, Q. The formation mechanism and exploration significance of ultra-deep, low-porosity and tight sandstone reservoirs in Kuqa depression, Tarim Basin. *Acta Pet. Sin.* **2014**, *35*, 1057. [CrossRef]
6. Zeng, L.; Song, Y.; Liu, G.; Tan, X.; Xu, X.; Yao, Y.; Mao, Z. Natural fractures in ultra-deep reservoirs of China: A review. *J. Struct. Geol.* **2023**, *175*, 104954. [CrossRef]
7. Wang, J.; Yang, X.; Zhang, J.; Wang, K.; Zhang, R.; Wang, Q.; Ren, B.; Ukar, E. Subsurface fracture characterization in a folded ultra-deep tight-gas sandstone reservoir: A case study from the Keshen gas field, Tarim Basin, China. *J. Struct. Geol.* **2023**, *172*, 104867. [CrossRef]
8. Chen, D.; Zhang, C.; Yang, M.; Li, H.; Wang, C.; Diwu, P.; Jiang, H.; Wang, Y. Research on water invasion law and control measures for ultradeep, fractured, and low-porosity sandstone gas reservoirs: A case study of Kelasu gas reservoirs in Tarim Basin. *Processes* **2024**, *12*, 310. [CrossRef]
9. Li, X.; Wang, Y.; Gu, J.; Yu, Z.; Yang, X.; Chang, Y.; Lu, A. Research and Practice on Liquid Extraction in Late Water Flooding of Ultra Deepwater Facies Sandstone Reservoirs. In Proceedings of the International Field Exploration and Development Conference 2023, Wuhan, China, 20–22 September 2023; Springer: Singapore, 2023; pp. 1775–1784. [CrossRef]
10. Zhang, D.; Kang, Y.; Selvadurai, A.P.S.; You, L.; Tian, J. The role of phase trapping on permeability reduction in an ultra-deep tight sandstone gas reservoirs. *J. Pet. Sci. Eng.* **2019**, *178*, 311–323. [CrossRef]
11. Wang, F.; Kobina, F. The Influence of Geological Factors and Transmission Fluids on the Exploitation of Reservoir Geothermal Resources: Factor Discussion and Mechanism Analysis. *Reserv. Sci.* **2025**, *1*, 3–18. [CrossRef]
12. Wu, J.; Ansari, U. From CO_2 Sequestration to Hydrogen Storage: Further Utilization of Depleted Gas Reservoirs. *Reserv. Sci.* **2025**, *1*, 19–35. [CrossRef]
13. Persoff, P.; Pruess, K. Two-phase flow visualization and relative permeability measurement in natural rough-walled rock fractures. *Water Resour. Res.* **1995**, *31*, 1175–1186. [CrossRef]
14. Fang, F.; Shen, W.; Gao, S.; Liu, H.; Wang, Q.; Li, Y. Experimental study on the physical simulation of water invasion in carbonate gas reservoirs. *Appl. Sci.* **2017**, *7*, 697. [CrossRef]
15. Shen, W.; Xu, Y.; Li, X.; Huang, W.; Gu, J. Physical simulation of water influx mechanism in fractured gas reservoirs. *J. Cent. South Univ. Sci. Technol.* **2014**, *45*, 3283–3287.
16. Johnson, E.F.; Bossler, D.P.; Bossler, V.O.N. Calculation of relative permeability from displacement experiments. *Trans. AIME* **1959**, *216*, 370–372. [CrossRef]
17. Babadagli, T.; Raza, S.; Ren, X.; Develi, K. Effect of surface roughness and lithology on the water–gas and water–oil relative permeability ratios of oil-wet single fractures. *Int. J. Multiph. Flow* **2015**, *75*, 68–81. [CrossRef]

18. Beltrán, A.; Hernández-Díaz, D.; Chávez, O.; García, A.; Mena, B.; Zenit, R. Experimental study of the effect of wettability on the relative permeability for air–water flow through porous media. *Int. J. Multiph. Flow* **2019**, *120*, 103091. [CrossRef]
19. Yacoub, A.; Djerbi, A.; Fen-Chong, T. The effect of the drying temperature on water porosity and gas permeability of recycled sand mortar. *Constr. Build. Mater.* **2019**, *214*, 677–684. [CrossRef]
20. Guo, P.; Zhang, H.; Du, J.; Wang, Z.; Zhang, W.; Ren, H. Study on gas-liquid relative permeability experiments of fractured-porous reservoirs. *Petroleum* **2017**, *3*, 348–354. [CrossRef]
21. Guo, X.; Zou, G.; Wang, Y.; Wang, Y.; Gao, T. Investigation of the temperature effect on rock permeability sensitivity. *J. Pet. Sci. Eng.* **2017**, *156*, 616–622. [CrossRef]
22. Chen, F.; Duan, Y.; Wang, K. Productivity Model Study of Water-Bearing Tight Gas Reservoirs Considering Micro-to Nano-Scale Effects. *Processes* **2024**, *12*, 1499. [CrossRef]
23. Li, J.; Liu, L.; Zhu, Y.; Zhao, L.; Chai, X.; Tian, L. A new dynamic model of supply boundary at low pressure in tight gas reservoir. *Sci. Rep.* **2025**, *15*, 12178. [CrossRef]
24. Lu, C.; Qin, X.; Ma, C.; Yu, L.; Geng, L.; Bian, H.; Zhang, K.; Zhou, Y. Investigation of the impact of threshold pressure gradient on gas production from hydrate deposits. *Fuel* **2022**, *319*, 123569. [CrossRef]
25. Yang, J.; Chen, W.; Tian, H.; Yu, H. Study of permeability evolutions in low permeability media under different stresses and temperatures. *Rock Soil Mech.* **2009**, *30*, 3587–3594. [CrossRef]
26. Fang, J.; Guo, P.; Xiao, X.; Du, J.; Dong, C.; Xiong, Y.; Long, F. Gas-water relative permeability measurement of high temperature and high pressure tight gas reservoirs. *Pet. Explor. Dev.* **2015**, *42*, 92–96. [CrossRef]
27. Li, Y.L.; Li, X.P.; Wu, F.; Lu, H.; Lei, X.; Wang, W.; Lu, R.; Li, J.; Tan, X. Experimental study on stress sensitivity of high-temperature and high-pressure sandstone gas reservoirs in Yingqiong Basin. *Energy Sci. Eng.* **2020**, *8*, 4116–4125. [CrossRef]
28. Mao, W.; Yao, Y.; Qin, Z.; Liu, Y.; Han, J.; Liu, Z. Pore structure characterization of sandstone under different water invasion cycles using micro-CT. *Geomech. Geophys. Geo-Energy Geo-Resour.* **2024**, *10*, 53. [CrossRef]
29. Yang, D.; Xie, K.; Lu, X.; Hu, Y.; Chen, F.; Jiao, C.; Jia, N.; Shen, W. Mechanisms of permeability alteration during water invasion in unconsolidated sandstone gas reservoirs. *Phys. Fluids* **2025**, *37*, 043312. [CrossRef]
30. Zhou, L.; Fan, X.; He, Y.; Gou, S.; Bi, Q.; Chen, J.; Chen, L.; Wang, J.; Guo, H.; Wu, Y.; et al. Enhanced the permeability of water invasion sandstone by effectively inhibiting the swelling and dispersion of montmorillonite. *J. Mol. Liq.* **2023**, *372*, 121196. [CrossRef]
31. Yan, Q.; He, Q.; Wei, L.; Qu, Z.; Ren, X. A laboratory study on percolation characteristics of single phase flow in low-permeability reservoirs. *J. Xi'An Pet. Inst.* **1990**, *5*, 1–6.
32. Li, A.; Zhang, S.; Liu, M.; Wang, W.; Zhang, L. A new method of measuring starting pressure for low permeability reservoir. *J. China Univ. Pet.* **2008**, *32*, 68–72.
33. Yang, Z.; Li, X.; Liu, S.; Gao, S. Threshold pressure effect of low permeability tight gas reservoirs in Sulige gas field. *Acta Pet. Sin.* **2015**, *36*, 347. [CrossRef]
34. Ding, J.; Yang, S.; Cao, T.; Wu, J. Dynamic threshold pressure gradient in tight gas reservoir and its influence on well productivity. *Arab. J. Geosci.* **2018**, *11*, 783. [CrossRef]
35. Hu, A.; Su, L.; Cao, G.; Luo, Z.; Yan, C.; Chen, Q. Experimental Study on the Effect of Fractures on the Irreducible and Movable Water in Water-Bearing Tight Sandstone Gas Reservoirs. *Processes* **2025**, *13*, 1685. [CrossRef]
36. Li, Y.; Fu, J.; Yan, W.; Chen, K.; Ding, J.; Wu, J. Experimental study on the dynamic threshold pressure gradient of high water-bearing tight sandstone gas reservoir. *Front. Earth Sci.* **2024**, *12*, 1487433. [CrossRef]
37. Tian, W.; Li, A.; Ren, X.; Josephine, Y. The threshold pressure gradient effect in the tight sandstone gas reservoirs with high water saturation. *Fuel* **2018**, *226*, 221–229. [CrossRef]
38. Li, S.; Cheng, L.; Li, X.; Hao, F. Nonlinear seepage flow of ultralow permeability reservoirs. *Pet. Explor. Dev.* **2008**, *35*, 606–612. [CrossRef]
39. Song, H.; Cao, Y.; Yu, M.; Wang, Y.; Killough, J.E.; Leung, J. Impact of permeability heterogeneity on production characteristics in water-bearing tight gas reservoirs with threshold pressure gradient. *J. Nat. Gas Sci. Eng.* **2015**, *22*, 172–181. [CrossRef]
40. Yao, J.; Ding, Y.; Sun, H.; Fan, D.; Wang, M.; Jia, C. Productivity analysis of fractured horizontal wells in tight gas reservoirs using a gas–water two-phase flow model with consideration of a threshold pressure gradient. *Energy Fuels* **2023**, *37*, 8190–8198. [CrossRef]
41. Zafar, A.; Su, Y.L.; Li, L.; Fu, J.-G.; Mehmood, A.; Ouyang, W.-P.; Zhang, M. Tight gas production model considering TPG as a function of pore pressure, permeability and water saturation. *Pet. Sci.* **2020**, *17*, 1356–1369. [CrossRef]
42. Lei, W. Exact analytical solutions for moving boundary problems of one-dimensional flow in semi-infinite porous media with consideration of threshold pressure gradient. *J. Hydrodyn. Ser. B* **2015**, *27*, 542–547. [CrossRef]
43. Zhu, W.; Song, H.; Huang, X.; Liu, X.; He, D.; Ran, Q. Pressure characteristics and effective deployment in a water-bearing tight gas reservoir with low-velocity non-Darcy flow. *Energy Fuels* **2011**, *25*, 1111–1117. [CrossRef]

44. Zhu, W.; Zou, G.; Liu, Y.; Liu, W.; Pan, B. The influence of movable water on the gas-phase threshold pressure gradient in tight gas reservoirs. *Energies* **2022**, *15*, 5309. [CrossRef]
45. Du, J.; Liu, Q.; Guo, P.; Jiang, T.; Xiong, Y.; Jiang, X. Study on water displacing gas relative permeability curves in fractured tight sandstone reservoirs under high pressure and high temperature. *ACS Omega* **2020**, *5*, 7456–7461. [CrossRef] [PubMed]
46. Mo, F.; Du, Z.; Peng, X.; Liang, B.; Tang, Y.; Yue, P. Analysis of Pressure-Dependent Relative Permeability in Permeability Jail of Tight Gas Reservoirs and its Influence on Tight Gas Production. *J. Porous Media* **2019**, *22*, 1667–1683. [CrossRef]
47. Khalaf, M.S.; Soliman, N.; El-Banbi, A.H. Wellbore storage removal in pressure transient analysis for gas wells. *J. Pet. Sci. Eng.* **2022**, *208*, 109712. [CrossRef]

Disclaimer/Publisher's Note: The statements, opinions and data contained in all publications are solely those of the individual author(s) and contributor(s) and not of MDPI and/or the editor(s). MDPI and/or the editor(s) disclaim responsibility for any injury to people or property resulting from any ideas, methods, instructions or products referred to in the content.